The microstructure of post-irradiated A508-3 steel and its effects on charpy impact energy

Lu Wu, Wei Zhang, Shaoyu Qiu, Xiaoyong Wu, Zhen Wang, Wen He, Bang Wen, Haisheng Zhang and Huajun Mo

Nuclear Power Institute of China, Sichuan, China
Corresponding author: Lu Wu <wulu1002@gg.com>

Irradiation hardening and embrittlement of reactor pressure vessel (RPV) steels, which is a key issue for the safety and lifetime assessment of nuclear reactors, are the consequence of microstructural changes under neutron irradiation (Mazouzi et al., 2011; Azevedo 2011; Little 1986; Terentyev et al., 2015). To apply Chinese A508-3 steel into RPVs, extensive research on its mechanical properties relevant to nuclear power plant environment has been carried out. The previous results of Charpy V-notch impact test reveals that the impact energies of post-irradiated A508-3 steel in the same test environment were unstable.

In order to find the possible reasons causing the instability of Charpy impact energy in A508-3 steel, the microstructure, grain size, defects, and non-metallic inclusions of post-irradiated specimens were observed by using optical microscope (OM), scanning electron microscope (SEM), and energy dispersive spectrometer (EDS) with shield in this paper. The results indicated that no obviously change in the bainite structure and grain size of the domestic A508-3 steel could be observed by OM under this irradiate conditions (fluence of neutron is 2.97×10^{19} n/cm^2, and irradiation temperature is 290℃±15℃), which could not lead to impact energy abnormally. Instead, the direct reason probably is the differences in fraction volume of the defects(cavities) in the matrix, which formed during solidification process. In addition, the defects could be divided into two types, one is filled with layer-like Al_2O_3, MnS, and Al-Mg-O ternary non-metallic inclusions combining together, and the other is voids. Furthermore, the boundary between these non-metallic inclusions and matrix is quite loose, which is easily to decrease the impact toughness. Otherwise, except MnS phase, the morphology and composition of the Al_2O_3 and Al-Mg-O ternary non-metallic inclusions in defects were not modified by neutron irradiation significantly under this irradiate conditions.

Experimental specimens

Detailed information of each sample is shown in Table 3.

Table 3: The results of impact testing

Specimens	Irradiation temperature T（℃）	Fluence （n/cm^2）	Impact temperature （℃）	Impact energy E（J）
1#	290±15	0	24	263
2#	290±15	2.97×10^{19}	0	213
3#	290±15	2.97×10^{19}	0	8

Results and Discussion

In order to analyze the inclusions and cavities in further, and confirm the effect of cavities on impact energy, the unirradiated and post-irradiated samples were analyzed by SEM and EDS. Figure 36 Figure 36 is the SE and BSE images, and X-ray mapping results of the inclusions in 1# unirradiated sample. As shown in Figure 36a, the inclusions exhibit irregular island-like morphology. Combine with the BSE image and X-ray mapping results in Figure 36, it is easy to find that three kinds of inclusions grow together as an ensemble. Based on EDS results, these inclusions (indicated by arrows A in Figure 36a, and B and C in Figure 36 b)have the compositions equivalent to Al_2O_3, $MgAl_2O_4$ (Reshak et al., 2014) and MnS respectively, which are commonly reported in A508-3 steels. In addition, some Ca, Cu, Mo, and Si atoms are dissolved inside the MnS inclusion. Furthermore, although these inclusions combine together very tightly, the boundary between these non-metallic inclusions and matrix is quite loose, which is easily to decrease the impact toughness.

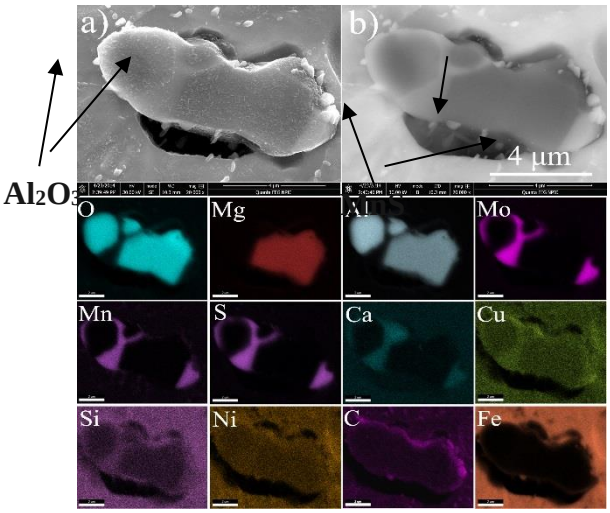

Figure 36: Secondary electron a), backscattered electron b) images and X-ray mapping results for non-metallic inclusions of Sample 1

The SEM images and X-ray mapping results of inclusions in 2# and 3# post-irradiated samples is presented Figure 37 and Figure 38 respectively. The Al2O3 and MgAl2O4 inclusions still could be observed after neutron irradiation. Compare with that, the MnS inclusion is absent Little 1986). In addition, there is no obviously differences in chemical composition between unirradiated and post-irradiated samples in the MgAl2O4 inclusion. But for the Al2O3 inclusion, after neutron irradiation, some Ca atoms(approximately 3.6 to 3.7 at.%) were dissolved inside. At the same time, the concentration of Al element in phase decreased from about 43.5 to 40.0 at.%. Furthermore, compare with Figures 36, 37 and 38, it seems that the Ca atoms which previously dissolved in MnS phase transfer into Al2O3 phase during irradiation process. However, mechanism of the transfer behavior of Ca atoms needs further investigation.

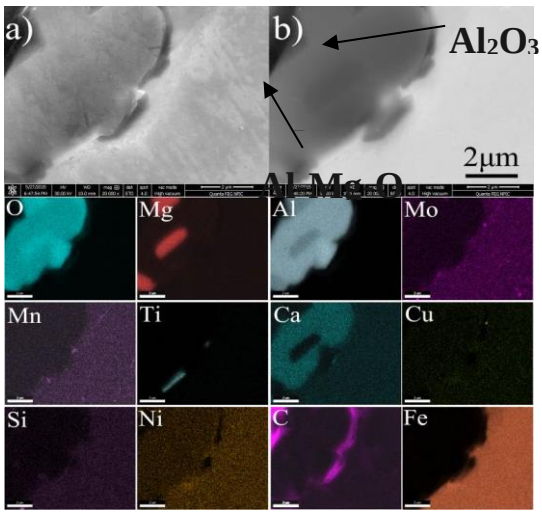

Figure 37: Secondary electron a), backscattered electron b) images and X-ray mapping results for non-metallic inclusions of Sample 2

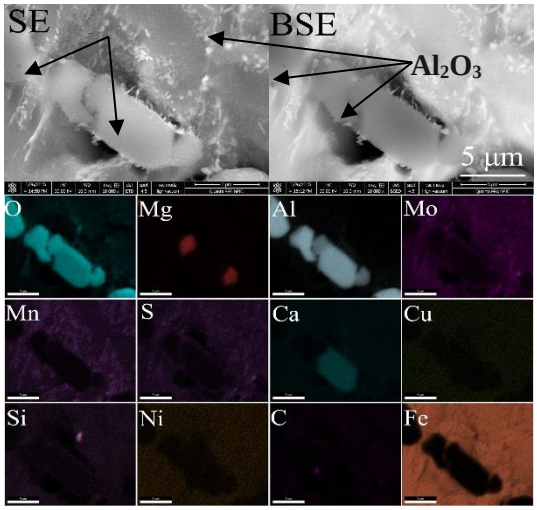

Figure 38: Secondary electron a), backscattered electron b) images and X-ray mapping results for non-metallic inclusions of Sample 3

References

Al Mazouzi, A., Alamo, A., Lidbury, D., Moinereau, D., & Van Dyck, S. (2011). PERFORM 60: Prediction of the effects of radiation for reactor pressure vessel and in-core materials using multi-scale modelling–60 years foreseen plant lifetime. *Nuclear Engineering and Design*, *241*(9), 3403-3415.

Azevedo, C. R. F. (2011). A review on neutron-irradiation-induced hardening of metallic components. *Engineering Failure Analysis*, *18*(8), 1921-1942.

Little, E. A. (1986). Fracture mechanics evaluations of neutron irradiated type 321 austenitic steel. *Journal of Nuclear Materials*, *139*(3), 261-276.

Reshak, A. H., Khan, S. A., & Alahmed, Z. A. (2014). Investigation of electronic structure and optical properties of MgAl2O4: DFT approach. *Optical Materials*, *37*, 322-326.

Terentyev, D., He, X., Bonny, G., Bakaev, A., Zhurkin, E., & Malerba, L. (2015). Hardening due to dislocation loop damage in RPV model alloys: Role of Mn segregation. *Journal of Nuclear Materials*, *457*, 173-181.